Identification of a Unique Cationic Impurity in Preladenant™ Using Accurate MS and NMR

Wendy Zhong,[a]* Bruce Hilton,[a] Gary Martin,[a] Lijun Wang,[b] and Shiuhang Henry Yip[b]

[a]Department of Global Analytical Chemistry, Merck Research Laboratories, Summit, New Jersey 07901
[b]Department of Process Chemistry, Merck Research Laboratories, Rahway, New Jersey 07065
*E-mail: wenqingzhong@yahoo.com

Received April 14, 2011
DOI 10.1002/jhet.1027
Published online 12 April 2013 in Wiley Online Library (wileyonlinelibrary.com).

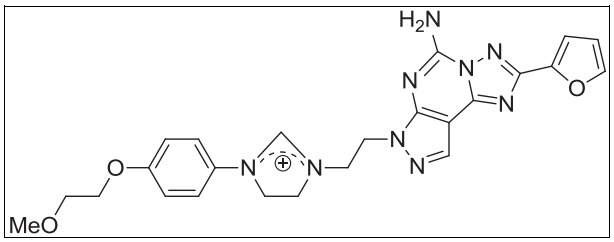

High resolution MS, 1D, and 2D NMR were used to determine the structure of a unique cationic impurity generated during the synthesis of Preladenant™ H/D exchange experiments were performed by both MS and NMR to confirm the acidic nature of the cationic dihydroimidazole proton. The presence of three exchangeable protons was established by MS experiments and the disappearance of the C11 proton in ^{1}H-NMR spectrum on equilibration with D_2O confirmed the acidic nature of the cationic dihydroimidazole proton. A piperazine ring contraction mechanism is proposed for the formation of the cationic dihydroimidazole.

J. Heterocyclic Chem., **50**, 281 (2013).

INTRODUCTION

Elucidation of the structures of impurities is an important step in refining process chemistry to develop a robust route for the manufacture of the active pharmaceutical ingredient (API) [1]. High resolution mass spectrometry provides accurate mass data that can determine the elemental composition of the unknown compounds [2–4]. Subsequent MS/MS experiments can then give more detailed structural information based on the fragment ions. 1D and 2D NMR can provide the information regarding the atom-to-atom connectivity through bonds and through space. Combining these two technologies, one can quickly and accurately determine impurity structures and identify degradation processes that have occurred during chemical synthesis and/or stability studies.

Preladenant™ (**1**) is an A2a receptor antagonist in late stage clinical trials that offers considerable promise in the treatment of Parkinson's disease [5–8]. Determination of the structures of unknown impurities in the A2a receptor antagonist's intermediate and final API is crucial for the optimization of the commercial synthetic route. Armed with the knowledge of impurity structures, reaction conditions can be optimized to reduce or to preferably eliminate their formation. The combined application of mass spectrometry and NMR spectroscopy facilitated the characterization of the structure of a unique impurity (**2**), generated during the synthesis of Preladenant, and enriched *via* forced degradation (see Experimental section). This impurity/degradant was also observed during a forced degradation study of Preladenant by LC/MS/MS experiments reported in 2010 [9]. The structure proposed for an impurity/degradant at m/z 488 was potentially incorrect. Misinterpretation of a fragment ion at m/z 430 most likely is attributed to a lack of the accurate MS/MS data leading to the subsequent misassignment of the structure. We now wish to revise the structure of this degradation product/synthetic impurity (referred to as an "impurity" throughout the article) at m/z 488. Extensive fragmentation pathways reported in an earlier study of **1** provided a strong foundation to quickly elucidate this structure [10]. Detailed structural analysis of 1D and 2D NMR spectra confirmed the proposed structure. H/D exchange experiments conducted by both MS and NMR provided additional confirmation of the cationic dihydroimidazolium moiety contained in the structure of **2**.

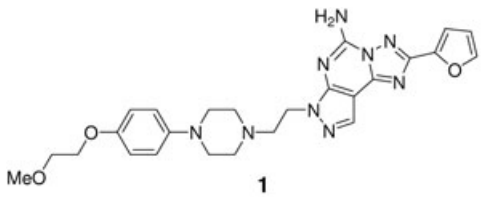

1

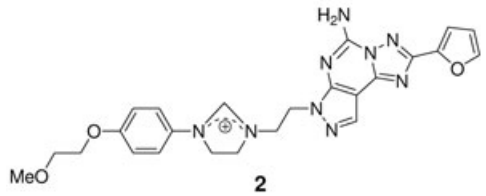

2

RESULTS AND DISCUSSION

The positive ion mass spectrum of the impurity is shown in Figure 1. The measured accurate mass of the precursor ion of this impurity is m/z 488.21353, which corresponds to an empirical formula of $C_{24}H_{26}N_9O_3$ $[M]^+$, with an error of −3.65 ppm between the measured accurate mass and calculated exact mass. It is worth noting that no sodium or other adduct ions were observed in the positive ion spectrum. By comparing the molecular formula of the unknown impurity with the API, $C_{25}H_{30}N_9O_3$ $[M+H]^+$, it is clear that the molecular formula of the unknown impurity at m/z 488 shows a loss of CH_3 compared with the API. The empirical formula data, however, cannot answer the question of the position in the structure where the modification occurred.

MS/MS experiments were next conducted to obtain additional structural information. For comparison purposes, MS/MS experiments were performed for the API at m/z 504. Figure 2 shows the MS/MS spectra of the protonated molecule of the API at m/z 504. The most abundant fragment ion at m/z 263 was the result of the cleavage of the C-N bond with a neutral loss of a 7***H***-pyrazolo[4,3-*e*][1,2,4] triazolo-[1,5-*c*]pyrimidin-5-yl amine moiety (Scheme 1). The fragment ion at m/z 311 was the product of a piperazine ring opening with a neutral loss of the methoxy-phenetole and a portion of the piperazine ring. The fragmentation pathway of m/z 504 was readily obtained based on the accurate mass MS/MS data as shown in Scheme 1. MS/MS experiments of the sodiated API molecule at m/z 526 were also conducted (not shown). The major fragment ion at m/z 467 is the result of a neutral loss of methoxyethane radical moiety (molecular formula of C_3H_7O.) from the m/z 526 as shown in Scheme 2.

Figure 3 shows the MS/MS spectrum of the unknown impurity at m/z 488. The major fragment ion at m/z 247, which corresponds to the fragment ion at m/z 263 in the API, was the result of the neutral loss of 7***H***-pyrazolo [4,3-*e*][1,2,4]triazolo-[1,5-*c*]pyrimidin-5-yl amine moiety.

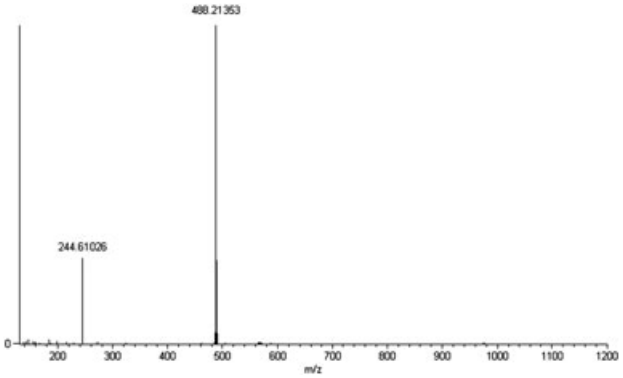

Figure 1. Positive ion mass spectrum of the unknown impurity, **2**, at m/z 488.

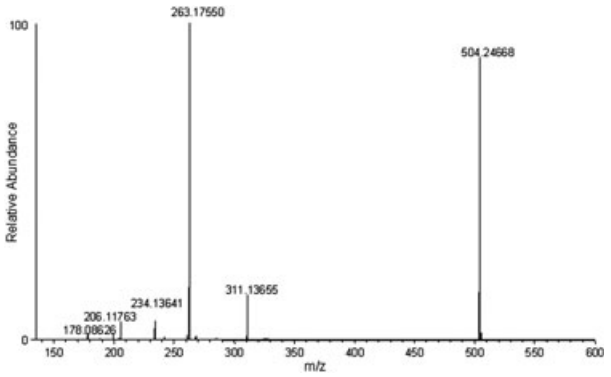

Figure 2. MS/MS spectrum of the protonated molecule, **1**, at m/z 504 obtained from Orbitrap MS.

In addition, the fragment ion at m/z 268 with the molecular formula of $C_{12}H_{10}N_7O^+$ was also present in the MS/MS spectra of the API as shown in Scheme 1. These two fragment ions suggest that the heterotricyclic moiety as shown below was present and intact in the impurity structure. The structural modification is not in this part of the molecule as shown by **3**.

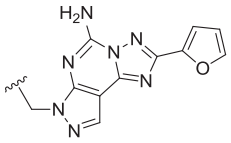

The fragment ion at m/z 430 with a molecular formula of $C_{21}H_{20}N_9O_2^+$ results from the neutral loss of a fragment with an empirical formula of C_3H_6O, which corresponds to methoxyethane. This fragment ion corresponds to the fragment ion at m/z 467 in the sodiated molecule of the API at m/z 526. Furthermore, the fragment ion at m/z 189 in the MS/MS spectrum of the unknown molecule at m/z 488 could be the further dissociation of the fragment ion at m/z 247 by losing the methoxyethene moiety. These data suggested that the methoxyethene/methoxyethane moiety is present in the unknown molecule.

The accurate mass data and the MS/MS fragmentation data strongly implicated the piperazine ring in the side chain of the molecule as the site of chemical modification relative to the API molecule. The cationic structure, **2**, was proposed based on the accurate mass and MS/MS data.

Comparison of the ^{1}H- and ^{13}C-NMR reference spectra of the impurity isolate with those of the API allowed the assignment of the majority of the resonances to be made on the basis of chemical shift considerations with the exception of the segment of the molecule from N10-C15 (see Fig. 4). Resonances

Scheme 1. The proposed fragmentation pathway of the protonated molecule, **1**, at m/z 504 based on the MS/MS data.

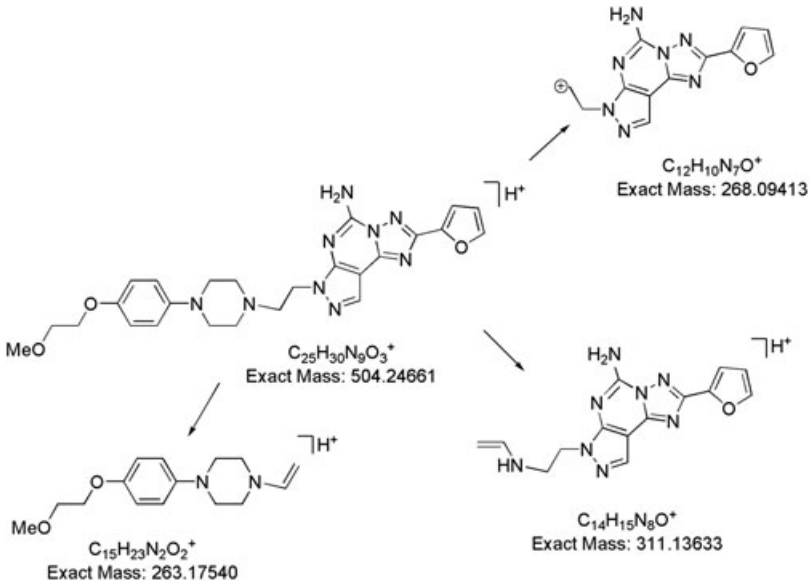

Scheme 2. The proposed fragmentation pathway of the sodiated molecule, **1**, at m/z 526 based on MS/MS data.

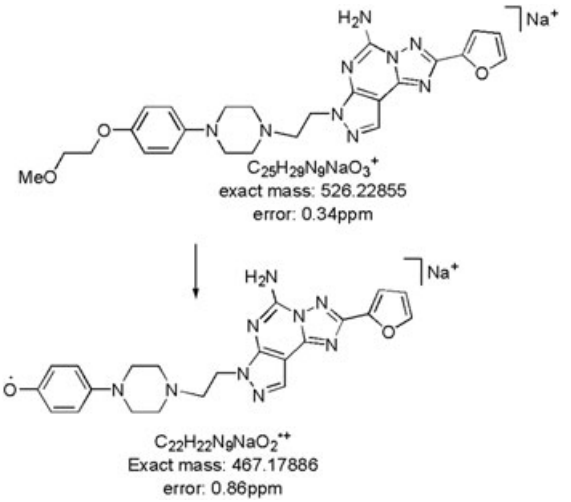

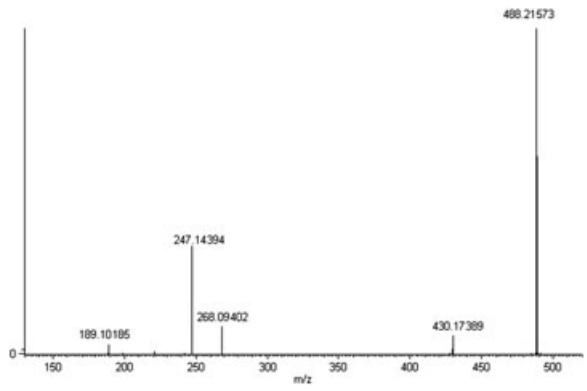

Figure 3. MS/MS spectrum of the unknown impurity, **2**, at m/z 488.

remaining to be assigned included a pair of methylene resonances from an ethylene bridge ($^1H/^{13}C$ 4.35/48.4 and 4.21/47.9 ppm) and a sp^2 methine resonance (8.81/154.9 ppm).

All three proton/carbon moieties show ^1H-^{13}C and long-range ^1H-^{15}N correlations to each other and to the adjacent atoms in the molecular structure. The NMR data support the conclusion that the two halves of the molecule are connected by a cationic dihydroimidazole ring as shown by **2** rather than the piperazine ring of **1**. The molecule has a net positive charge. In comparison with structure **1**, the chemical shifts of the central ring nitrogens have shifted considerably downfield (N10, shifted from 55.7 to 137.1 ppm; and N13 shifted from 33.3 to 128.2 ppm. In contrast, the N18 and N19 resonances shifted only slightly (N18 shifted from 186.0 to 187.1 ppm and N19 shifted from 300.8 to 302.7 ppm). Furthermore the predicted chemical shifts using ACD™ for N10 and N13 are markedly different from the observed values if, as is required by the prediction program, the positive charge is placed

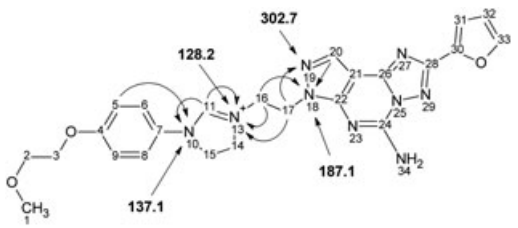

Figure 4. Numbered structure of **2**. Arrows show long-range 1H-15N GHMBCAD correlations. The inset table shows the chemical shifts for the various nitrogen resonances calculated using the NNMR.

on a single nitrogen atom. The observed ^{15}N chemical shifts suggest that the most plausible explanation of the data is that the positive charge is delocalized across both nitrogens of the imidazole ring and the nitrogen chemical shifts of N10 and N13 represent an average of the predicted chemical shifts in molecules with a single positively charged nitrogen.

The chemical shifts of H11 (8.81 ppm) and C11 (154.9 ppm) are also consistent with the proposed cationic dihydroimidazole ring structure. The proton NMR spectrum also showed that ^{13}C satellites flanking the H11 resonance corresponding to $^{1}J_{CH}$ = 206 Hz. This coupling constant is consistent with a sp^2 carbon flanked by two nitrogen atoms, as shown by **2**. The $^{1}J_{CH}$ coupling constant of C11 is quite similar to that of the 2-position of pyrimidine, (203 Hz) and the 3- or 5-positions of 1***H***-1,2,4-triazole, (205 Hz). [11]

Calculated and assigned ^{1}H, ^{13}C, and ^{15}N chemical shifts for **2** are collected in Table 1. ^{13}C and ^{15}N chemical shifts for **2** were calculated using the CNMR and NNMR programs v11.01, respectively, provided by ACD Laboratories.

H/D exchange studies. As noted above, no sodium or other adduct ions were observed in the positive ion spectrum of **2**, which is typical of cationic small molecules. Furthermore, cationic molecules are not always observed in negative ion mass spectrometry. However, as shown in Figure 5, a molecular ion for **2** was observed at m/z 486, which corresponds to the deprotonated mass of the impurity. The proposed cationic dihydroimidazole moiety can be inferred to be acidic in nature, therefore, in the negative ion mode, it could logically deprotonate to the form as shown in structure **4**. Consequently, the 11-position should undergo H/D exchange.

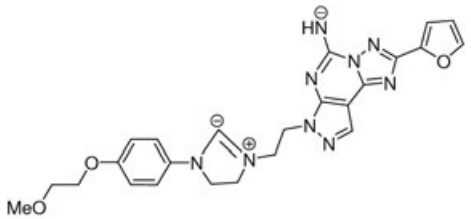

Chemical Formula: $C_{24}H_{24}N_9O_3^-$
Exact Mass: 486.20076

4

H/D exchange experiments were performed to test this hypothesis. Figure 6 shows the positive ion spectrum of **2** after H/D exchange. The measured accurate mass for the deuterated molecule is m/z 491.23274, which corresponds to an empirical formula of $C_{24}H_{23}D_3N_9O_3$ $[M]^+$ with an error of −2.86 ppm. The MS data confirm that there are three exchangeable protons in this molecule. Typically, a gain of three deuterons would equate to two exchangeable

Table 1

Collected ^{1}H, ^{13}C, and ^{15}N NMR data obtained for sample **2** in DMSO-d_6.

Assignment	$\delta^{1}H$ (ppm)	multiplicity, *J* (Hz)	δ ^{13}C (ppm)	δ ^{15}N (ppm)
1	3.26	s	58.8	–
2	3.59	cm	70.0	–
3	4.00	cm	67.0	–
4	–	–	156.9	–
5/9	7.06	d 9.0	119.0	–
6/8	6.94	d 9.0	115.2	–
7	–	–	129.3	–
10	–	–	–	137.1
11	8.81	s	154.9	–
13	–	–	–	128.2
14	4.35	dd 10.3, 11.2	48.4	–
15	4.21	dd 10.3, 11.2	47.9	–
16	4.02	dd 3.7, 6.6	47.5	–
17	4.64	t 4.3	43.3	–
18	–	–	–	187.1
19	–	–	–	302.7
20	8.26	s	132.5	–
21	–	–	96.0	–
22	–	–	149.1	–
23	–	–	–	not obs
24	–	–	148.7[a]	
25	–	–	–	not obs
26	–	–	145.2[a]	
27	–	–	–	not obs
28	–	–	155.4	
29	–	–	–	not obs
30	–	–	146.6[a]	
31	7.22	d 3.2	112.2	–
32	6.74	dd 3.3, 1.9	112.1	–
33	7.95	s, broad	145.2	–
34	8.15	s, broad	–	not obs

Abbreviations: s, singlet; d, doublet; t, triplet; q, quartet; cm, complex multiplet.
[a]Assignments may be interchanged.

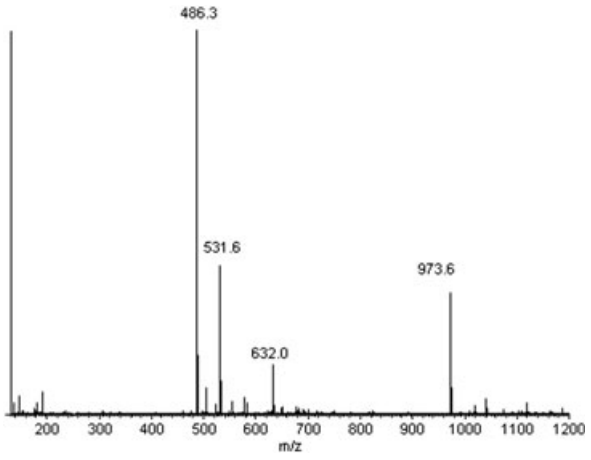

Figure 5. The negative ion mass spectrum of the unknown impurity, **2**, performed in linear trap portion.

protons and an ionizing deuteron. However, in the case of a cationic molecule, the number of deuterons gained in the H/D exchange experiment corresponds to the number of exchangeable protons [12–14]. Since the NMR data below are consistent with this molecule's cationic nature, in this specific example, the number of deuterons gained corresponds directly to the number of exchangeable protons.

MS/MS experiments were performed on the deuteriated form of the unknown impurity, **2**, at m/z 491 ion, affording the fragmentation pathways, which was compared with the fragmentation pathways of the protonated form of **2** at m/z 488 shown in Scheme 3. The side-by-side comparison of the fragmentation patterns affords a clear understanding of where the exchangeable protons reside. The fragment ion at m/z 430 from the protonated form shifted three Daltons higher to m/z 433 in the deuterated form, which is consistent with the incorporation of three deuterons based on the molecular formula derived from the accurate mass data. Similarly, the fragment ion at m/z 268 in the protonated form shifted two Daltons higher to m/z 270 in the deuterated form, consistent with the incorporation of two deuterium atoms. The most important information is derived from the m/z 247 and m/z 189 fragment ions in the protonated form, both of which were shifted one Dalton higher to m/z 248 and 190, respectively, in the deuterated form. These data provide direct support of the acidic nature of the cationic dihydroimidazole moiety.

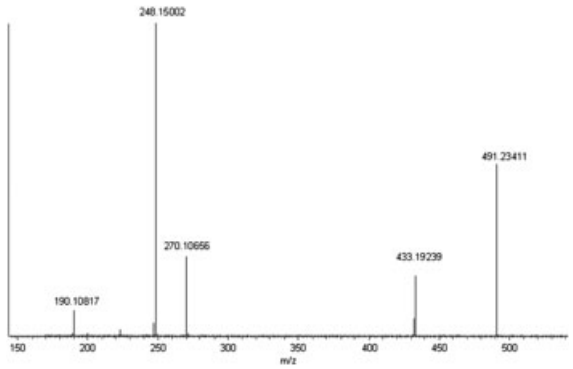

Figure 6. MS/MS spectrum of the deuterated unknown impurity, **2**, at m/z 491.

To further substantiate the location of the deuterium exchange of the H11 proton, 60 μL of D_2O was added to the NMR sample and the proton spectrum was reacquired after 48 h of equilibration. The H11 resonance observed at 8.81 ppm was completely absent from the proton NMR spectrum, indicating that it had undergone deuterium exchange. This observation strongly supports the proposed acidity of the H11 proton.

The cationic impurity formation could be attributed to piperazine ring contraction, which has been reported previously [15]. Scheme 4 shows a plausible mechanism of the dihydroimidazolium impurity **2** formation through an oxidation pathway proposed based on the few precedents available [15–17]. Oxidation of piperazine possibly by oxygen (from solvent or air) under heated acidic conditions can generate diformamide **5**. One of the formamido groups of **5** is hydrolyzed to yield **6**. The remaining formamide on **6** can be envisioned to undergo nucleophilic attack by the adjacent nitrogen to give rise to intermediate **7**,

Scheme 3. The proposed fragmentation pathways of the cationic (deuteriated) impurity, **2**, at m/z 488 (m/z 491), are shown above.

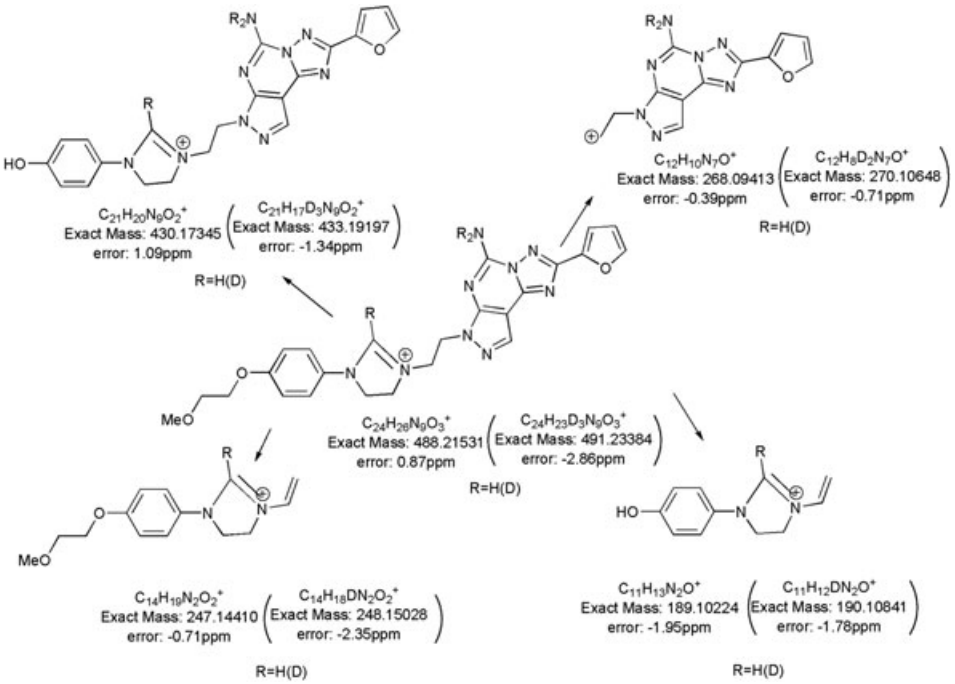

which, in turn, loses a molecule of water to form the dihydroimidazolium impurity, **2**. Additionally, isolation and identification of another impurity 8 [9], a result of losing both CO moiety from **3**, supports the ring contraction mechanism proposed.

CONCLUSIONS

Concerted interpretation of the MS and NMR data has conclusively shown that the piperazine ring of **1** underwent ring contraction to afford the dihydroimidazolium moiety contained in the structure of **2**. The dihydroimidazolium specie accounts for the observed chemical shift of the H11/C11 resonant pair and the significant downfield shift of the N10 and N13 ^{15}N resonances. The proposed structure also explains the $^{1}J_{CH}$ coupling constant for C11 and the acidity of the position as reflected by the H/D exchange studies performed.

EXPERIMENTAL

Enrichment and isolation of the cationic impurity. A solution of Preladenant (**1**, 10 g), acetonitrile (110 mL), water (85 mL), and 37% HCl (2 mL) was heated at 75°C for 15 days. The resulting mixture was added drop wise to a mixture of water (30 mL), acetonitrile (6.5 mL), and 25% NaOH (3 mL) to crystallize Preladenant. The resulting slurry was filtered and then washed with water and acetonitrile. The filtrate was extracted with EtOAc (2 × 25 mL). The combined extracts were concentrated to give 1.2 grams of solids. The solids obtained contained ~17% of **2**. The solids were dissolved in acetonitrile and purified with a YMC ODS-A column (250 × 6mm, 5μm) eluted with 60/40 0.1% TFA in water/ACN in water (3:1) (Flow rate: 1 mL/min; run time: 19 min). The desired fractions were concentrated to provide purified **2** for further MS and NMR studies.

Mass spectrometry. LC/MS experiments were conducted using a Thermo LTQ™-Orbitrap instrument equipped with a Surveyor HPLC system. The high resolution LC/MS and LC/MS^n spectra were acquired in the FTMS mode using an Orbitrap instrument at a resolution of 30,000 (at m/z 400) to determine the elemental composition of each fragment ion. The electrospray ionization needle was held at 4.5 kV, and a nitrogen sheath gas and a nitrogen auxiliary gas were used to stabilize the spray. The heated capillary was set at 270°C. All MS/MS experiments were conducted in the linear ion trap. Helium was introduced into the ion trap to improve the trapping efficiency and also serve as the collision gas for CID. The operational pressure after introducing helium was ~2×10^{-5} Pa in the linear ion trap.

LC gradient conditions were 20% B to 100% B in 15 min at the flow rate of 200 μL/min. Mobile phase compositions were: (A) 95% HPLC grade H_2O (10 m*M* NH_4OAc)/5% ACN, and (B) 5% H_2O (10 m*M* NH_4OAc)/95% ACN. The sample was eluted using an XTerra C18 MS HPLC column, 2.1 × 150 mm, with 3.5 μm particle size. The sample was dissolved in ACN at the concentration of 1 mg/mL with the injection volume of 5 μL. H/D exchange experiments were conducted *via* direct infusion and the sample was dissolved in ACN/D_2O with the concentration of 0.5 mg/mL. The sample was introduced through ESI source at a flow rate of 5 mL/min.

NMR spectroscopy. A sample was prepared for NMR analysis by dissolving a 1 mg sample in ~200 μL of d_6-DMSO (CIL), after which the sample was transferred to a 3 mm NMR tube (Wilmad) using a flexible Teflon™ needle and a Hamilton gas-tight syringe. The majority of the NMR

Scheme 4. A proposed formation mechanism of the cationic dihydroimidazole impurity (**2**) through an oxidation pathway.

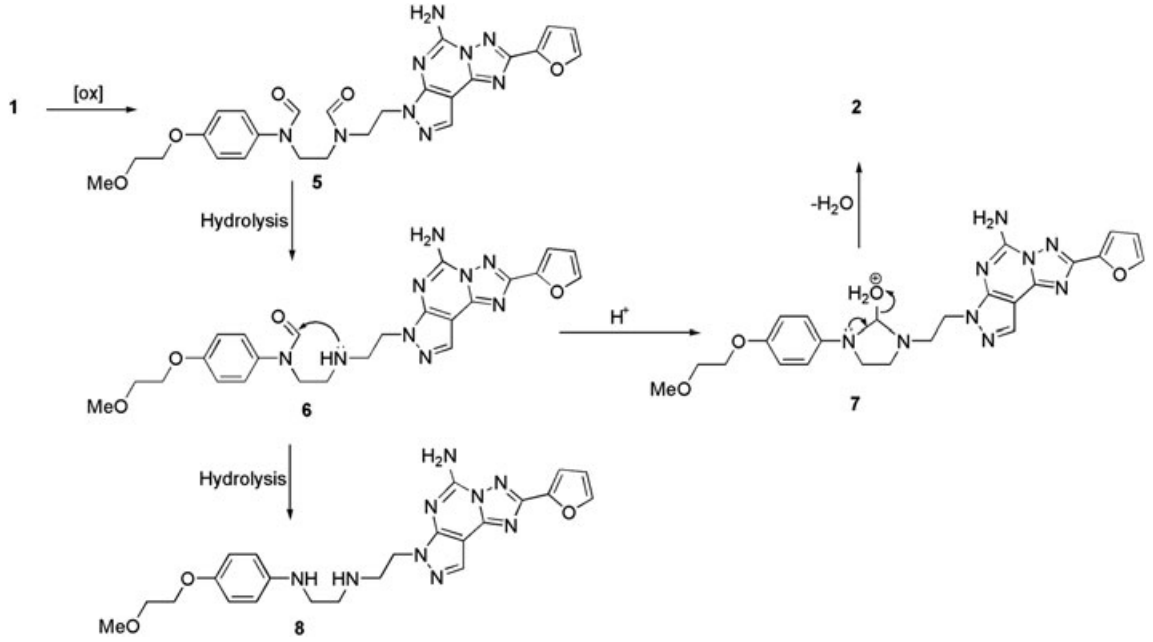

experiments were performed on a Varian 600 MHz NMR spectrometer equipped with a 5 mm Varian ColdProbe™ operating at an RF coil temperature of 20 K. All data were collected with the sample temperature controlled at 20°C. The proton NMR data acquired consisted of a proton reference spectrum, a GCOSY spectrum, and a 400 ms ROESY spectrum; the heteronuclear 2D NMR spectra acquired consisted of multiplicity edited ^{1}H-^{13}C GHSQCAD, an 8 Hz optimized ^{1}H-^{13}C GHMBCAD spectrum, and a 6 Hz optimized ^{1}H-^{15}N GHMBCAD spectrum. A ^{13}C reference spectrum was acquired using a Varian 500 MHz NMR spectrometer equipped with a ^{13}C-^{1}H dual probe.

REFERENCES AND NOTES

[1] Martin, G. E. In Analysis of Drug Impurities; Smith, R. J., Webb, M. L., Eds.; Blackwell Publishing: Oxford, 2007; p 124.

[2] Feng, X.; Siegel, M. M. Anal Bioanal Chem 2007, 389, 1341.

[3] Guan, S.; Marshall, A. G.; Scheppele, S. E. Anal Chem 1996, 68, 46.

[4] Tong, H.; Bell, D.; Tabei, K.; Siegel, M. M. J Am Soc Mass Spectrom 1999, 10, 1174.

[5] Salamone, J. D. IDrugs 2010, 13, 723.

[6] Hodgson, R. A.; Bedard, P. J.; Varty, G. B.; Kazdoba, T. M.; Di Paolo, T.; Grzelak, M. E.; Pond, A. J.; Hadj Tahar, A.; Belanger, N.; Gregoire, L.; Dare, A.; Neustadt, B. R.; Stamford, A. W.; Hunter, J. C. Exp Neurol 2010, 225, 384.

[7] Kuo, S.; Tsai, D. J.; Tran, L. T.; Zhang, P.; Jones, A. D. U.S. Pat. Appl Publ 2005, 15 pp.

[8] Neustadt, B. R.; Hao, J.; Lindo, N.; Greenlee, W. J.; Stamford, A. W.; Tulshian, D.; Ongini, E.; Hunter, J.; Monopoli, A.; Bertorelli, R.; Foster, C.; Arik, L.; Lachowicz, J.; Ng, K.; Feng, K.-I. Bioorg Med Chem Lett 2007, 17, 1376.

[9] Zhang, L. K.; Pramanik, B. N. J Mass Spectrom 2010, 45, 146.

[10] Zhong, W.; Irish, P. A.; Martin, G. E. J Heterocyclic Chem 2009, 46, 591.

[11] Breitmaier, E.; Voelter, W. Carbon-13 NMR Spectroscopy, 3rd ed.; VCH: New York, 1987; p 145.

[12] Zhong, W.; Yang, J. Rapid Commun Mass Spectrom 2009, 23, 3255.

[13] Novak, T. J.; Helmy, R.; Santos, I. J Chromatogr B 2005, 825, 161.

[14] Ohashi, N.; Furuuchi, S.; Yoshikawa, M. J Pharm Biomed Anal 1998, 18, 325.

[15] Doss, G. A.; Miller, R. R.; Zhang, Z.; Teffera, Y.; Nargund, R. P.; Palucki, B.; Park, M. K.; Tang, Y. S.; Evans, Y. S. D. C.; Baillie, T. A.; Stearns, R. A. Chem Res Toxicol 2005, 18, 271.

[16] Petride, H.; Draghici, C.; Florea, C.; Petride, A. Cent Eur J Chem 2006, 4, 674.

[17] Feng, W.; Liu, H.; Chen, G.; Malchow, R.; Bennett, F.; Lin, E.; Pramanik, B.; Chan, T.-M. J Pharm Biomed Anal 2001, 25, 545.

1

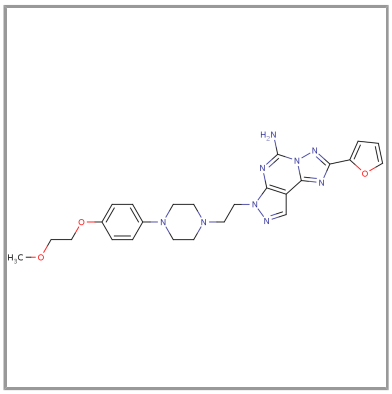

Compound Details Structure Search

2

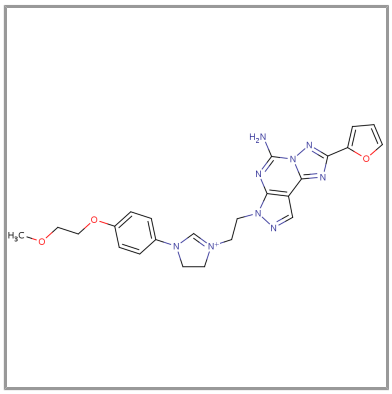

Compound Details Structure Search

3

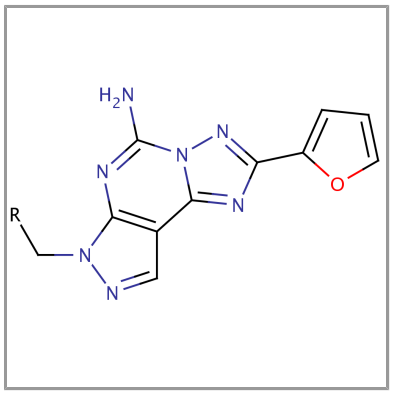

Compound Details Structure Search

4

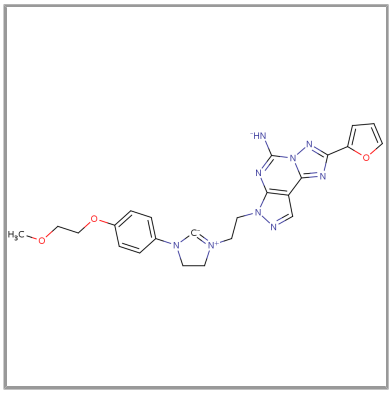

Compound Details Structure Search